PAPR Reduction in FBMC Systems Using Phase Realignment based Techniques

Robin Shrestha and Jong-Soo Seo
Dept. of Electrical and Electronics Engineering
Yonsei University, Seoul, S. Korea 120-749.
Email: {robinsth, jsseo}@yonsei.ac.kr

***Abstract*—Recently, filter bank multicarrier (FBMC) has been given a huge interest as an alternative to orthogonal frequency division multiplexing (OFDM). FBMC scheme has increased frequency efficiency and low out-of-band (OOB) emission as compared with OFDM. However, FBMC still suffers from a high peak-to-average power ratio (PAPR) as in OFDM systems. Several OFDM based PAPR reduction techniques have been adopted for FBMC system. In this paper, novel techniques for PAPR reduction for FBMC systems are proposed based on the evolution of the phase realignment (PR) and modified PR (MPR) techniques used for OFDM systems. The proposed PAPR reduction techniques are designed to improve the PAPR performance at the cost of minimal degradation of the bit error rate (BER) performances, defined by a transmit error vector magnitude (EVM). Unlike other existing techniques, the proposed techniques reduce the average power of the FBMC symbols, which help to retain low BER per unit energy. Simulation results show the proposed techniques as the potential alternative for PAPR reduction in FBMC systems.**

***Keywords*—FBMC/OQAM; PAPR; PR; MPR; EVM; BER;**

I. Introduction

Filter bank multicarrier (FBMC) has received increasing interest in systems like cognitive radio and opportunistic dynamic spectrum access. It is highly probable to be considered as a viable replacement to orthogonal frequency division multiplexing (OFDM). FBMC was introduced [1] as an alternative to OFDM and has improved spectral efficiency and low out-of-band (OOB) radiation. Well localized waveforms provide flexible usage of the resources in both domains as well as aid in increasing computational complexity. However, the complexity can be greatly reduced by using a polyphase implementation [2].

In spite of the major advantage of FBMC over OFDM, the FBMC systems also have a major disadvantage of high peak-to-average power ratio (PAPR) of the transmitted signal. Due to the overlapping structure of FBMC signals, the PAPR reduction techniques used for OFDM systems cannot be used directly for FBMC systems. Several of the conventional OFDM PAPR reduction techniques (like [3], [4]) are adopted for FBMC systems.

There have been several researches that focus on the PAPR reduction of FBMC systems [5]–[8]. A PAPR reduction technique for FBMC based on active constellation extension (ACE) with projection-onto-convex-sets (POCS) and smart gradient project (SGP) are discussed in [5]. The ACE has a considerable PAPR reduction, but increases the average transmit power, which either decrease in the power efficiency or degrades the BER performance [5]. Clipping and filtering (CF) based techniques have a high PAPR reduction, but have worse BER performance, requiring a sophisticated noise cancellation technique at the receiver. An overview and evaluation of clipping based iterative PAPR reduction techniques for FBMC are presented in [9]. The PTS [6] and SLM [7] both have a good PAPR reduction, however, they introduce high complexity to the system and may require the side information to be transmitted. In [8], a PAPR reduction scheme based on extending candidate transmit sequence is presented, where the linear combination of the candidate transmit sequences are extended considering the overlapping property between adjacent symbols in FBMC systems.

In this paper, we propose two PAPR reduction techniques for FBMC systems, namely, phase realignment (PR) and modified phase realignment (MPR). The PR and MPR have been proposed and experimented in OFDM systems in our previous work [3], [4]. Like ACE, PR modifies the constellation points over the data subcarriers of the CF signal in the frequency domain. In FBMC, the offset quadrature amplitude modulation (OQAM) is used, where the in-phase and quadrature components of QAM symbols have a shift of half the symbol period. The proposed techniques convert the OQAM symbols back to QAM symbol to process it. In PR, the phase of the CF constellation is restored back to its original phase and the amplitude is limited within a specific amplitude margin from the amplitude of the conventional M-QAM. While in MPR, a phase margin is introduced in addition to the amplitude margin. The phase of the CF constellation point beyond the allowable phase margin is restored to the respective phase threshold defined by the phase margin. The shortcoming of the PR and MPR is acceptable degradation in BER performance, which would be nominal due the effect of both the reduced PAPR and the reduced average transmit power.

II. System Model

We consider a typical FBMC system with N subcarriers that are modulated using OQAM[1]. The system takes a set of input data bits $\mathbf{a} = [a_1 a_2 ... a_{N \log_2 M}]$, which are modeled using the M-QAM symbols $X_m[n] = \alpha_m[n] + j\beta_m[n]$, where $\alpha_m[k]$ and $\beta_m[k]$ are the real and imaginary parts of

This work has been supported by the Institute of BioMed-IT, Energy-IT and Smart-IT Technology (BEST), a Brain Korea 21 plus program, Yonsei University. This research was funded by the ICT R&D program of MSIP/IITP (1391202006, A Study on Next Generation Interactive Terrestrial Broadcasting System).

[1]FBMC is used to indicate FBMC with OQAM symbols.

the complex symbol on the n-th subcarrier of m-th FBMC symbol. The complex M-QAM symbols are mapped into the I/Q channel baseband symbol based on OQAM modulation. Finally, prior to transmission, the symbols are overlapped.

The discrete-time FBMC signal $s[k]$ can be expressed based on the complex M-QAM symbol $X_m[n]$ as the n-th subcarrier during the m-th time slot as shown below,

$$x[k] = \sum_{m=-\infty}^{\infty} \sum_{n=0}^{N-1} (\theta_n \alpha_m[n] p_0[k - mN] + \theta_{n+1} \beta_m[n] p_0[k - mN]) e^{jn(k-mN)\frac{2\pi}{N}} \ \forall k \in [1, ..., N], \quad (1)$$

where θ_n is 1 for even n and j ($j = \sqrt{-1}$) for odd n, and N is the total number of available subcarriers. $p_0[\cdot]$ is the prototype filter of finite length, which is associated with the overlapping ratio of the consecutive FBMC symbols.

The PAPR is an important metric in multicarrier transmission schemes. It is used to describe the fluctuation of a signal. The PAPR of the m-th FBMC symbol can be obtained by [5],

$$PAPR_m = \frac{\max |x[mN + k]|^2}{\mathbb{E}[|x[mN + k]|^2]}, \quad k \in [0, 1, ..., N-1], m \in [0, 1, ..., \bar{M}/2]. \quad (2)$$

where $\mathbb{E}[\bullet]$ denotes the expectation operator, K is an overlapping factor, and $\bar{M}$ is the total number of FBMC symbol transmitted.

The PAPR reduction capability may be evaluated by using the complementary cumulative distribution function (CCDF). The CCDF is defined as the probability that the PAPR of a FBMC signal exceeds a given threshold Γ and is given by

$$CCDF[PAPR_m] = Pr[PAPR_m > \Gamma]. \quad (3)$$

The power amplifier typically used for terrestrial and mobile communication is a solid state power amplifier (SSPA). The complex RF output, which is nonlinearly distorted can be expressed as

$$\begin{aligned} y(t) &= A(\rho(t)) e^{j\{\phi(t) + \Phi(\rho(t))\}} \\ &= Y(\rho(t)) e^{j\phi(t)}, \end{aligned} \quad (4)$$

where $\rho(t)$ and $\phi(t)$ are the amplitude and phase of the input signal. $A(\bullet)$ and $\Phi(\bullet)$ are the AM/AM and the AM/PM conversion of the nonlinear distortion, respectively, and $Y(\rho(t)) = A(\rho(t)) e^{j\Phi(\rho(t))}$ is the complex soft envelop of the amplified signal $y(t)$. The SSPA model is usually modeled using Rapp's model as

$$\begin{aligned} A[\rho(t)] &= \frac{\rho(t)}{\left[1 + \left(\frac{\rho(t)}{x_{sat}}\right)^{2p}\right]^{1/2p}}, \text{ and} \\ \Phi[\theta(t)] &= 0, \end{aligned} \quad (5)$$

where x_{sat} is a parameter that sets the output saturation level and p is a parameter that controls the AM/AM sharpness of the saturation region. The AM/AM characteristics becomes similar to that of the soft limiter as $p \to \infty$.

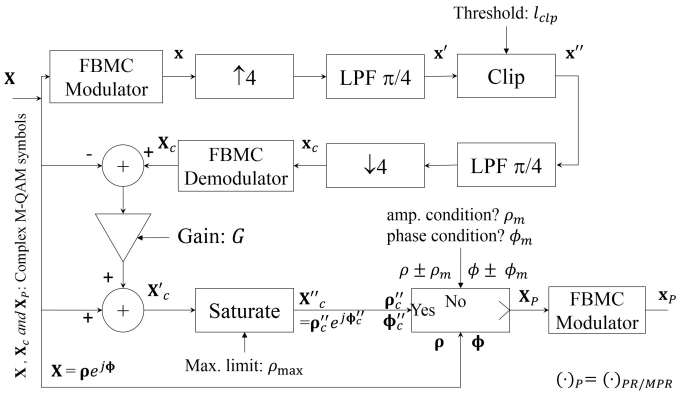

Fig. 1. Implementation of the PR/MPR in FBMC system.

III. Phase realignment based PAPR reduction technique

In this section, we propose a simple non-bijective[2] constellation mapping technique of PAPR reduction in FBMC systems based on the realignment of the phase of the CF constellation point, namely PR and MPR. The PR has been introduced in our previous work [3] and MPR in [4] for OFDM systems.

The PR and MPR are implemented right after CF and FBMC demodulation on each FBMC symbol in the frequency domain as shown in Fig. 1. As shown in the figure, the proposed techniques produce a time domain signal $\mathbf{x}_p$ ($\mathbf{x}_{PR}$ or $\mathbf{x}_{MPR}$) that replaces the original signal $\mathbf{x} = [x_0, x_1, ..., x_{N-1}]$ obtained by performing FBMC modulation on a set of frequency domain values $\mathbf{X} = [X_0, X_1, ..., X_{N-1}]$. It is to be noted that the $\mathbf{X}$ is a vector of N complex M-QAM symbols. The FBMC modulator performs the polyphase implementation of FBMC, which includes the OQAM processing and mapping of the input vector, IFFT operation, and prototype filtering; and the reverse in the FBMC demodulator. $\mathbf{x}$ is oversampled and filtered to obtain $\mathbf{x}' = [x'_0, x'_1, ..., x'_{N-1}]$ before clipping operation. The clipping operation is defined as follows

$$x''_k = \begin{cases} x'_k, & \text{if } ||x'_k|| \le l_{clp} \\ l_{clp} \cdot \frac{x'_k}{||x'_k||}, & \text{otherwise,} \end{cases} \quad (6)$$

where $\mathbf{x}'' = [x''_0, x''_1, ..., x''_{N-1}]$ is the clipped signal and $l_{clp} = \sqrt{CR \cdot P_{av}}$ is the clipping threshold obtained by using the CR and the average power. The filtering, downsampling, and FBMC demodulation (including conversion to M-QAM symbol) are performed to obtain the CF signal in frequency domain, $\mathbf{X}_c$, which is further processed as

$$\mathbf{X}'_c = \mathbf{X} + G \cdot (\mathbf{X}_c - \mathbf{X}), \quad (7)$$

where $\mathbf{X}c - \mathbf{X}$ is the CF noise and G is the parameter to set the intensity of CF noise.

Now, the saturation operation is implemented on $\mathbf{X}'_c$ with the maximum amplitude threshold ρ_{max} to obtain $\mathbf{X}''_c = \rho''_c e^{-j\phi''_c}$ that avoids an excessive growth of the amplitude. Then, the conditions on the amplitude and phase of the CF constellation are imposed to obtain either the PR or MPR signal.

[2]Mapping done without using one-to-one transformation to form the desired output.

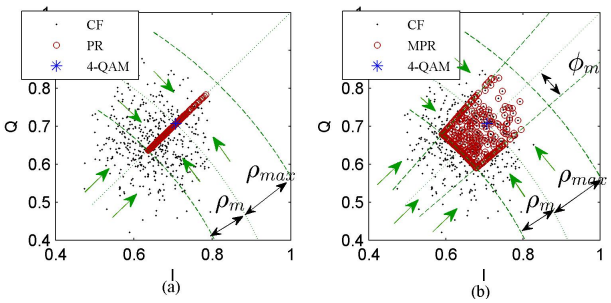

Fig. 2. Conceptual process in the first quadrant of 4-QAM constellation for (a) PR and (b) MPR.

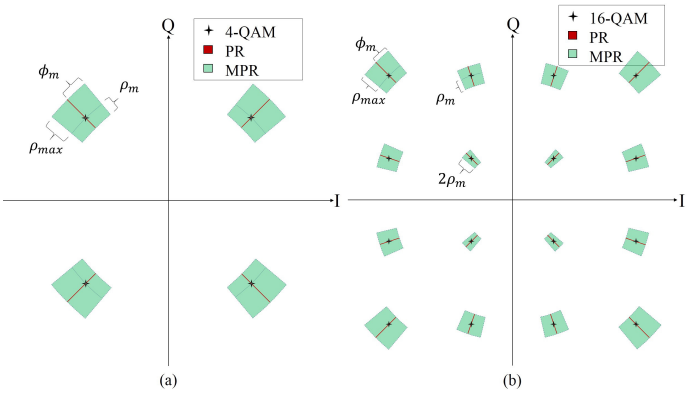

Fig. 3. Signal constellations after applying PR and MPR techniques; (a) 4-QAM, (b) 16-QAM.

A. Phase Realignment

In PR, the phase and the amplitude of the distorted signals are manipulated to achieve the low PAPR profile. As a consistence, there is a slight degradation of the BER performance, which often could be compensated as shown in [10]. The PAPR of the CF signal is low at a price of highly degraded BER performance. Careful restriction of the amplitude and phase of the CF signal to improve its BER performance would retain much of the signal property that contributes to low PAPR.

Following (7) and saturation operation, the phase $\phi_c'' = [\phi_c''(1), \phi_c''(2), ..., \phi_c''(N-1)]$ is realigned to its original state as was prior to CF, and the amplitude beyond the range of $\pm\rho_{\mathsf{m}}$ from the original amplitude is scaled to the respective margin. For the outermost constellation points in the corners and sides, the restriction on the outward extension is dropped. Considering the amplitude and phase of the input M-QAM modulated symbol $\mathbf{X} = \rho e^{j\phi}$ as $\rho = [\rho(1), \rho(2), ..., \rho(N-1)]$ and $\phi = [\phi(1), \phi(2), ..., \phi(N-1)]$, the amplitude ($\rho_{\mathbf{PR}}$) and the phase $\phi_{\mathbf{PR}}$) vectors for PR signal can be mathematically expressed respectively as

$$\rho_{PR}(n) = \begin{cases} \rho(n) + \rho_{\mathsf{m}}, & \text{if } \rho_c''(n) > \rho(n) + \rho_{\mathsf{m}} \\ \rho(n) - \rho_{\mathsf{m}}, & \text{if } \rho_c''(n) < \rho(n) - \rho_{\mathsf{m}} \\ \rho_c''(n), & \text{otherwise.} \end{cases} \quad (8)$$

and

$$\phi_{PR}(n) = \phi(n), \quad (9)$$

Thus, the PR signal in time domain $\mathbf{x}_{PR}$ can be obtained by using IFFT on $\mathbf{X}_{PR} = \rho_{PR} e^{-j\phi_{PR}}$.

The conceptual process of the PR can be easily explained using the constellation points in the first quadrant of 4-QAM before and after implementing the CF and PR as shown in Fig. 2 (a). The dashed arc represents the amplitude margin and the maximum amplitude threshold. The arrows indicate the direction in which the CF constellation point is shifted as the PR process is carried out.

B. Modified Phase Realignment

In PR, realigning the phase not only enhances the BER performance compared with the CF, but also regenerates peaks to increase the PAPR slightly. This can be solved by introducing a phase margin ϕ_{m} in addition to the amplitude margin ρ_{m}.

The MPR has the phase margin along with the amplitude margin. The phases of only those CF constellation points residing outside the allowable phase ($\phi \pm \phi_{\mathsf{m}}$) are changed to the respective phase boundary. This can be represented mathematically as

$$\phi_{MPR}(n) = \begin{cases} \phi(n) + \phi_{\mathsf{m}}, & \text{if } \phi_c''(n) > \phi + \phi_{\mathsf{m}} \\ \phi(n) - \phi_{\mathsf{m}}, & \text{if } \phi_c''(n) < \phi - \phi_{\mathsf{m}} \\ \phi_c''(n), & \text{otherwise,} \end{cases} \quad (10)$$

where $\rho_{\mathbf{MPR}}$ and $\phi_{\mathbf{MPR}}$ are the amplitude and phase vector of the MPR signal.

The concept of the MPR process is depicted in Fig. 2 (b). MPR process is similar to the PR process except that the phases of the CF constellation points are limited by the phase margin ($\pm\phi_{\mathsf{m}}$) along with its amplitude margin.

The resulting constellations by implementing PR and MPR are depicted in Fig. 3 for 4-QAM and 16-QAM.

It is to be noted that, even though the PR and MPR techniques decreases the minimum Euclidean distance of the constellation points, this does not necessarily degrade the BER performance. Both the PR and MPR have reduced average transmit power which can help retain the BER performance per unit energy.

C. Amplitude margin and phase margin

In this section, we determine the amplitude margin (ρ_{m}) and phase margin (ϕ_{m}) for the PR and MPR. The objective here is to reduce the PAPR such that the error vector magnitude (EVM) of the PR/MPR shall be within a predefined threshold ϵ. The optimization problem to determine appropriate ρ_{m} and ϕ_{m} can be mathematically represented as (see [4] for details).

$$\begin{aligned} &\min_{\phi_{\mathsf{m}}} \max_{n} |x(n)|^2 \\ &\text{subject to: } \rho_{\mathsf{m}} = \sqrt{(\epsilon \cdot S_{max}/100)^2 - \phi_{\mathsf{m}}^2} \\ &\qquad 0 \le \phi_{\mathsf{m}} \le \epsilon \cdot S_{max}/100, \end{aligned} \quad (11)$$

where S_{max} is the maximum amplitude of M-QAM signal and ϵ is the EVM threshold (in %). The problem is readily solved for the PR (setting $\phi_{\mathsf{m}} = 0$), whereas for the MPR, it can be easily solved by using techniques like random search.

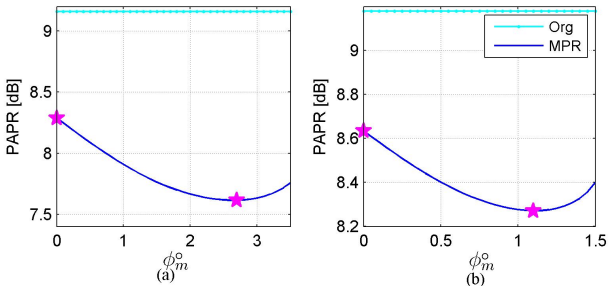

Fig. 4. PAPR vs. $\phi_{\mathsf{m}}^{\circ}$ ($\rho_{\mathsf{m}} = f(\epsilon, \phi_{\mathsf{m}}^{\circ})$) the MPR in FBMC M-QAM systems (a) $M = 16$, CR = 5.3 dB, $\epsilon = 5\%$; (b) $M = 64$, CR = 6.5 dB, $\epsilon = 1.8\%$.

TABLE I. OPTIMUM AMPLITUDE AND PHASE MARGINS FOR FBMC 16 AND 64-QAM

Modulation	CR	ϵ	PR (ρ_{m})	MPR ($\rho_{\mathsf{m}}, \phi_{\mathsf{m}}^{\circ}$)
16-QAM	5.3 dB	5%	0.0671	(0.0477, 2.7)
Average PAPR reduction			0.88 dB	1.56 dB
64-QAM	6.5 dB	1.8%	0.0275	(0.0197, 1.1)
Average PAPR reduction			0.55 dB	0.91 dB

IV. NUMERICAL RESULTS

In this section, we first obtain the optimal amplitude and phase margins $(\rho_{\mathsf{m}}, \phi_{\mathsf{m}})$ via numerical simulation and then evaluate the PAPR and BER performances of the proposed PR and MPR in comparison to the ACE-POCS and ACE-SGP. The gain G in proposed techniques is left for future experiment and is assumed to be one.

We consider FBMC system using the polyphase implementation and the PHYDYAS [2] prototype filter of $K = 4$. The total number of subcattier is 1024 out of which 854 subcarriers are used for data transmission. 16-QAM and 64-QAM modulation are used as a complex input symbol. A single iteration is used for both POCS and SGP in ACE. The FBMC system has the transmit block of length $\bar{M} = 40$. The HPA is modeled by using Rapp's model for $p = 3$. While the complexity of the proposed PR/MPR is similar to that of the ACE-POS, we evaluate the PAPR and BER performance as follows.

A. Optimization of the margins

The optimum amplitude and phase margins were obtained by solving (11). The optimum margin ρ_{m} for the PR is readily obtaining by putting $\phi_{\mathsf{m}}^{\circ}$. For MPR, we obtain the PAPR for various phase margins, $\phi_{\mathsf{m}}^{\circ}$[3] and obtain the optimum phase margin. Fig. 4 (a) and (b) depicts the PAPR of the MPR against the phase margins $\phi_{\mathsf{m}}^{\circ}$ in the FBMC 16- and 64-QAM systems, respectively. The EVM threshold ϵ were assigned as 5% and 1.8% for 16- and 64-QAM, respectively.

The optimum amplitude and phase margins for 16- and 64-QAM are listed in Table I.

B. PAPR Performance

The CCDFs of the proposed techniques are compared with those of ACE-POCS and ACE-SGP. The CCDF plots of the proposed PR and MPRs techniques along with others are depicted in Figs. 5 and 6 for 16- and 64-QAM, respectively. It can be seen that the CCDFs of both PR and MPR are consistently better than ACE-POCS for all modulation orders. On the other hand, CCDF of ACE-SGP is the best among various PAPR reduction techniques (nearly same as the CF) which is followed by the MPR. As the modulation order increases, PAPR performance slowly degrades for all the techniques. This is because all the techniques are based on the shaping of the CF in frequency domain for a given CR. When the modulation order increases the CR should be increased as well as the IBO. Upon increasing the CR, there is only a little room for the CF noise shaping based PAPR reduction techniques to improve the PAPR.

In ACE-SGP the outward projection of the constellation results in better PAPR performance, but only by increasing the average transmission power. In ACE-POS, the average power

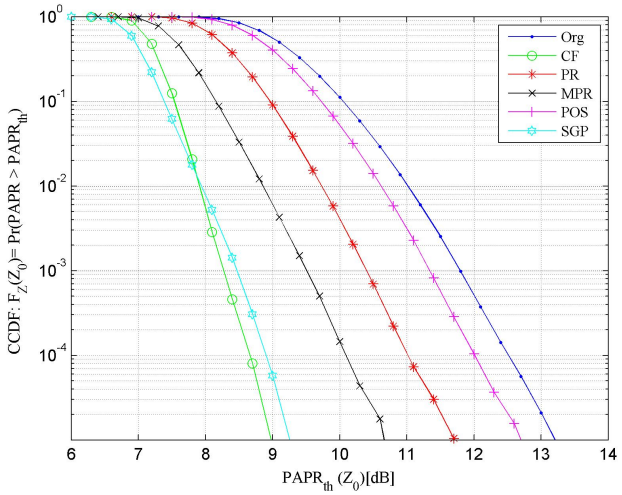

Fig. 5. CCDF of the PAPR for PR, MPR and other techniques applied to FBMC 16-QAM signal.

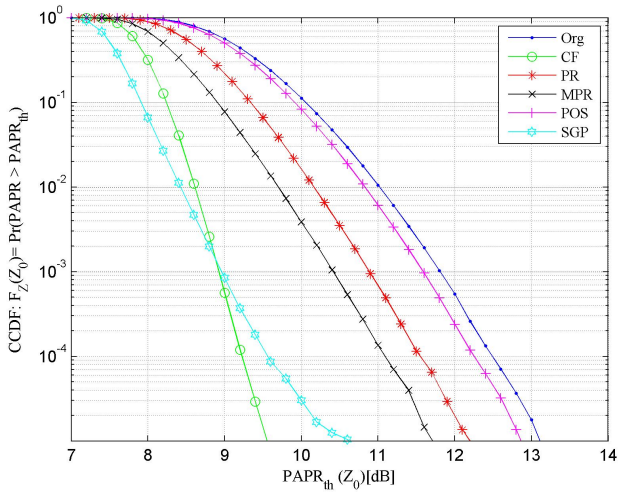

Fig. 6. CCDF of the PAPR for PR, MPR and other techniques applied to FBMC 64-QAM signal.

[3] $\phi_{\mathsf{m}}^{\circ}$ is the phase margin in degrees.

TABLE II. APPROXIMATE PAPR REDUCTIONS (dB) ACHIEVED BY VARIOUS PAPR REDUCTION TECHNIQUES FOR CCDF OF $1e-4$

Modulation	PR	MPR	ACE-POCS	ACE-SGP
16-QAM	1.5	2.4	0.5	3.4
64-QAM	1	1.6	0.2	3

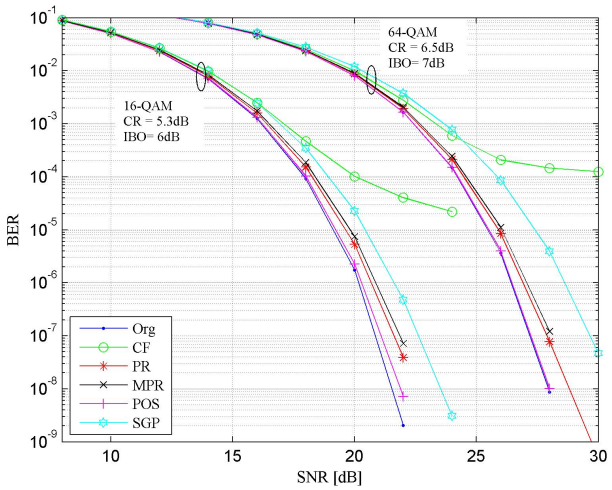

Fig. 7. BER performance of FBMC 16- and 64-QAM with various PAPR reduction techniques applied with Rapp's model ($p = 3$) of HPA under Rayleigh fading channel.

is further increased. Whereas in PR and MPR, many of the CF constellation points are left undamaged and the amplitude and phase margins are designed such that there are inward extensions of the constellation as well, thereby decreasing the average transmission power.

Based on the results in Figs. 5 and 6 the approximate PAPR reduction achieved by various techniques for the CCDF of $1e-4$ are listed in Table II.

C. BER performance

The BER performance of the proposed techniques, ACE-POCS, and ACE-SGP applied to FBMC M-QAM system are analyzed in conjunction with the Rapp's model ($p = 3$) of nonlinear HPA over Rayleigh fading channel. For a fair comparison, we consider normalizing all the systems to unit energy. The resulting plots are shown in Fig. 7 for 16- and 64-QAM, where it is observed that for BER of 1e-4, both PR and MPR have BER degradation of up to 0.7 dB. The BER performance of the ACE-SGP is the worst only second to the CF method because of the effect of the increased average transmission power. The BER degradation in ACE-SGP becomes more sever as the modulation order increases. The BER degradation of the proposed techniques can be reduced by lowering the EVM threshold ϵ, but it will also have effect on the PAPR performance.

V. CONCLUSION

In this paper, a new PAPR reduction technique called PR and its modified version MPR are proposed for FBMC systems. Our simulation results demonstrate that both the proposed techniques would be effective in reducing PAPR by up to 2.4 dB and 1.6 dB with BER degradation of less than 0.7 dB for FBMC 16- and 64-QAM, respectively. The MPR performs better than the PR and ACE-POS. The ACE-SGP has the highest PAPR reduction, which is close to that of CF method, but has highest BER degradation, only second to the CF method, due to the effect of increased average transmission power. Thus, we conclude that the MPR is a potential alternative for PAPR reduction that is effective in terms of PAPR reduction, implementation complexity, and BER degradation.

REFERENCES

[1] M. Bellanger, "Specification and design of a prototype filter for filter bank multicarrier transmission," *in Proc. IEEE Int. Conf. Acoustics, Speech, and Signal Process.*, Salt Lake City, USA, May 2001, pp.2417–2420.

[2] F. Schaich, "Filterbank based multi carrier transmission (FBMC); evolving OFDM: FBMC in the context of WiMAX," *in Proc. European Wireless Conf.*, Apr. 2010, pp.1051–1058.

[3] R. Shrestha, M. H. Seo, G. W. Go, and B. S. Lee, "PAPR reduction and Pre-distortion techniques against non-linear Distortion of Satellite WiBro," *in Proc. JC-SAT Conf.*, Busan, S. Korea, Nov. 2008

[4] R. Shrestha, J. M. Kim, and J. S. Seo, "Enhanced Phase Realignment Techniques for the PAPR Reduction in OFDM Systems,"unpublished. **

[5] V. D. Neut *et al.*, "PAPR reduction in FBMC systems using a smart gradient-projection active constellation extension method," *in Proc. Telecommunication, 2014 21st Int. Conf. on*, May 2014, pp. 134 – 139.

[6] C. Jose and S. M. Deepa, "Peak to Average Power Ratio Reduction and Inter Symbol Interference Cancellation of FBMC-OQAM signals," *International Journal of Engineering Research & Technology*, vol. 03, no. 03, pp. 1890 – 1894, Mar. 2014.

[7] G. Cheng, H. Li, B. Dong, and S. Li, "An Improved Selective Mapping Method for PAPR Reduction in OFDM/OQAM System," *Scientific Research: Communications and Network*, vol. 5, pp. 53–56, Sep. 2013.

[8] Z. He, J. Wang, X. Dy, J. Yan, and H. Xu, "A Novel PAPR Reduction Scheme in FBMC-OQAM Systems Based on Extend Candidate Transmit Sequences," *Journal of Information & Computational Science 12:3 (2015)*, 5, pp. 915– 925, Feb. 2015.

[9] Z. Kollar, L. Varga, B. Horvath, P. Bakki, and J. Bito, "Evaluation of Clipping Based Iterative PAPR Reduction Techniques for FBMC Systems," *The Scientific World Journal*, vol 2014, pp. 1 – 12, 2014.

[10] T. Jiang, C. Li, and C. Ni, "Effect of PAPR Reduction on Spectrum and Energy Efficiencies in OFDM Systems With Class-A HPA Over AWGN Channel," *IEEE Trans. Broadcast.*, vol. 59, no. 3, pp. 513–519, Sept. 2013.